Lipid rafts function in biosynthetic delivery of proteins to the cell surface in yeast

Michel Bagnat[†], Sirkka Keränen[‡], Anna Shevchenko[§], Andrej Shevchenko[§], and Kai Simons[†¶]

[†]Cell Biology Program and European Molecular Biology Laboratory, 69012 Heidelberg, Germany and Max Planck Institute for Molecular Cell Biology and Genetics, 01307 Dresden, Germany; [‡]VTT Biotechnology, P.O. Box 1500, FIN-02044 VTT, Finland; and [§]Peptide and Protein Group, European Molecular Biology Laboratory, 69012 Heidelberg, Germany

Contributed by Kai Simons, January 27, 2000

Lipid rafts, formed by lateral association of sphingolipids and cholesterol, have been implicated in membrane traffic and cell signaling in mammalian cells. Sphingolipids also have been shown to play a role in protein sorting in yeast. Therefore, we wanted to investigate whether lipid rafts exist in yeast and whether these membrane microdomains have an analogous function to their mammalian counterparts. We first developed a protocol for isolating detergent-insoluble glycolipid-enriched complexes (DIGs) from yeast cells. Sequencing of the major protein components of the isolated DIGs by mass spectrometry allowed us to identify, among others, Gas1p, Pma1p, and Nce2p. Using lipid biosynthetic mutants we could demonstrate that conditions that impair the synthesis of sphingolipids and ergosterol also disrupt raft association of Gas1p and Pma1p but not the secretion of acid phosphatase. That endoplasmic reticulum (ER)-to-Golgi transport of Gas1p is blocked in the sphingolipid mutant *lcb1–100* raised the question of whether proteins associate with lipid rafts in the ER or later as shown in mammalian cells. Using the *sec18–1* mutant we found that DIGs are present already in the ER. Taken together, our results suggest that lipid rafts are involved in the biosynthetic delivery of proteins to the yeast plasma membrane.

Asymmetric distribution of proteins and lipids depends on active sorting processes. The finding that in MDCK cells glycosphingolipids were sorted apically led to the proposal that glycosphingolipid clusters form platforms that mediate polarized delivery of proteins (1). These platforms or lipid rafts are thought to be formed by the tight packing of the long and highly saturated fatty acids of sphingolipids with cholesterol into which proteins specifically associate (2). The sphingolipid–cholesterol rafts can be considered to form a separate phase, a liquid-ordered phase segregating from the bulk liquid-disordered phase (3). The property of being insoluble in cold, nonionic detergents such as Triton X-100 (TX100) allows the purification of lipid rafts by floatation in density gradients in the form of detergent-insoluble glycolipid-enriched complexes (DIGs) (4). In mammalian cells, DIG association takes place at the level of the Golgi complex at which sphingolipids are synthesized (4, 5).

The integrity of DIGs depends on the presence of cholesterol and sphingolipids. When cholesterol is extracted from cells by using methyl-β-cyclodextrin (CD) and cholesterol biosynthesis is blocked by lovastatin, both DIG association and polarized delivery of influenza hemaglutinnin (HA), a marker for rafts, to the apical membrane of MDCK cells and to the axonal membrane of hippocampal neurons are impaired (5–7). Inhibition of sphingolipid synthesis with fumonisin B leads to missorting of glycosylphosphatidylinositol (GPI)-anchored GP-2 in MDCK cells (8) and increased detergent solubility and missorting of Thy1 and HA in hippocampal neurons (7).

In yeasts, lipids also are distributed asymmetrically. Glycosphingolipids and ergosterol are progressively enriched along the secretory pathway, reaching the highest levels at the plasma membrane (9). However, other compartments such as the vacuole exhibit a remarkably low ergosterol-to-phospholipid ratio and low levels of sphingolipids (10–12). These observations together with the fact that sphingolipids are required for endoplasmic reticulum (ER)-to-Golgi transport of GPI-anchored Gas1p but not for vacuolar CPY (13–15) suggest that glycosphingolipids and ergosterol are sorted to the cell surface and may form platforms, as their mammalian counterparts do, for the transport of proteins. Consistent with this idea, the presence of DIGs in yeasts has been reported (16).

In this work, we show the existence of functional lipid rafts in yeast composed of glycosphingolipids and ergosterol.

Materials and Methods

Media, Strains, and Plasmids. Yeast strains used in this work are: W303–1a (MAT**a** *ade2–1 trp1–1 can1–100 leu2–3 112, his3–11 15, ura3–1*), W303–1b (MATα *ade2–1 trp1–1 can1–100 leu2–3 112, his3-11 15, ura3–1*), RH3804 (MATα *lcb1–100 trp1 leu2 ura3 lys2 bar1*) (H. Riezman, University of Basel, Switzerland), RH690–15D (MAT**a** *his4 ura3 leu2 lys2 bar1*) (H. Riezman), H891 (MATα *trp1–289 leu2–3 112, ura3–52 his4–580 sec18–1*, large-colony variant of mBY12–16D of R. Schekman, University of California Berkeley, CA) (S. Keränen, VTT Biotechnology), FY14 (MATα *hem1 erg1*::*URA3 ade2 leu2*) (L. Parks, North Carolina State University, Raleigh, NC), and GL7 (MAT**a** *gal2 erg12–1 hem3–6*) (W. D. Nes, Texas Tech University, Lubbock, TX). Rich medium (yeast extract/peptone/dextrose) and minimal medium were prepared according to ref. 17. In the experiments using sterol auxotrophs, rich or minimal medium was supplemented with Tween 80 (1.5%) and ergosterol (10 μg/ml in methanol) or with ergosterol and/or ergosterol (5–10 μg/ml in Tergitol Nonidet P-40/ethanol, 1:1) and mixture of oleic and palmitoleic acids (4:1, vol/vol) (0.01% in Tergitol Nonidet P-40/ethanol, 1:1). Low-phosphate medium was prepared according to ref. 18. Labeling with [^{14}C]acetate (200 μCi/mmol; Amersham Pharmacia) was done in Na/K-Pi buffer (25 mM, pH 6.5) with 1% glucose. Nystatin (Sigma) was used at 10 μM. The human transferrin receptor (hTfR) was subcloned from pGEM1-TR into p2146 (ADH promoter from *Schizosaccharomyces pombe* inserted as a *Sph*I-to-*Eco*RI fragment in YCplac33 by using the *Eco*RI site.

DIG Isolation. Cells were grown at 30°C in rich medium to log phase, and 10–20 OD_{600} units were collected, washed once in water, and stored at −20°C. Then, the cell pellet was lysed in 500

Abbreviations: CD, methyl-β-cyclodextrin; DIGs, detergent-insoluble glycolipid enriched complexes; GPI, glycosylphosphatidylinositol; ER, endoplasmic reticulum; hTfR, human transferrin receptor; Nano ES MS/MS, nanoelectrospray tandem mass spectrometry; PLs, phospholipids; SLs, sphingolipids; TX100, Triton X-100; MALDI, matrix-assisted laser desorption ionization.

¶To whom reprint requests should be addressed at: European Molecular Biology Laboratory, Postfach 10.2209, D-69117 Heidelberg, Germany. E-mail: Simons@embl-Heidelberg.de.

The publication costs of this article were defrayed in part by page charge payment. This article must therefore be hereby marked "*advertisement*" in accordance with 18 U.S.C. §1734 solely to indicate this fact.

Article published online before print: *Proc. Natl. Acad. Sci. USA*, 10.1073/pnas.060034697. Article and publication date are at www.pnas.org/cgi/doi/10.1073/pnas.060034697

μl of TNE buffer (50 mM Tris·HCl, pH 7.4/150 mM NaCl/5 mM EDTA) with a protease inhibitor mixture (1 mM PMSF/2.5 μg/ml chymostatin, leupeptin, antipain, and pepstatin) by vortexing with glass beads two times for 5 min at 4°C. The lysate then was cleared of unbroken cells and debris by centrifugation at 500 × *g* for 5 min. The cleared lysate then was incubated with TX100 (1% final) for 30 min on ice. After the extraction with TX100, the lysate (250 μl) was adjusted to 40% Optiprep by adding 500 μl of Optiprep solution (Nycomed, Oslo) and overlaid with 1.2 ml of 30% Optiprep in TXNE (TNE/0.1% TX100) and 200 μl of TXNE. The samples were centrifuged at 55,000 rpm for 2 h in a TLS55 rotor (Beckman), and six fractions of equal volume were collected from the top. The top fraction was subjected to a second incubation with TX100, adjusted to 40% Optiprep, and overlaid with a step gradient (in TNE) and spun again in a TLS55 rotor as before. Fractions from the second gradient were collected from the top, precipitated by adding two volumes of 15% trichloroacetic acid, and analyzed by SDS/PAGE and silver staining or Western blotting.

Mass Spectrometry. Protein bands were visualized by staining with silver (19), and protein bands enriched in the top fraction were excised from the gel and in-gel-digested with trypsin (unmodified, sequencing grade; Boehringer Mannheim) (19). Proteins were identified by a combination of high-mass-accuracy matrix-assisted laser desorption ionization peptide mapping (MALDI MS) and nanoelectrospray tandem mass spectrometric sequencing (Nano ES MS/MS) as described (20). MALDI MS was performed on a modified REFLEX mass spectrometer (Bruker, Billerica, MA). Nano ES MS/MS was performed on an API III triple-quadrupole mass spectrometer (PE Sciex, Concord, Ontario, Canada) equipped with a nanoelectrospray ion source built at the European Molecular Biology Laboratory. Database searching was performed against a comprehensive, nonredundant sequence database by using PEPTIDESEARCH 3.0 software developed at the European Molecular Biology Laboratory. No limitations on protein molecular weights and species of origin were imposed.

Metabolic Labeling with [^{3}H]Inositol. Cells were grown to log phase in synthetic medium without inositol (B101,CA), and 7.5 OD_{600} units were resuspended in 2 ml of fresh medium and labeled for 1 h with 75 μCi of myo[2-^{3}H]inositol (20 Ci/mmol; Sigma) and chased for 1 h by diluting 4-fold with fresh medium.

Preparation of Total Membranes and Cyclodextrin Extraction. Total membrane fractions were prepared by floatation in density gradients. Cleared lysates were adjusted to 40% Optiprep and overlaid with 30% Optiprep (in TNE) and with TNE buffer. After centrifugation (2 h in a TLS55 rotor at 55,000 rpm or 4 h in a SW60 rotor at 28,000 rpm), the membrane fraction was recovered from the 30–0% interface. Extractions with CD (Sigma) were performed as described (21).

Lipid Analysis. For labeling phospholipids (PLs) and sphingolipids (SLs), cells were inoculated in 10 ml of low-phosphate medium at 0.003 OD_{600} and grown overnight to OD_{600} 1 at 30°C in the presence of 1 mCi of [^{32}P]orthophosphate (10 mCi/ml; Amersham Pharmacia). Then, radiolabeled cells were mixed with 40 OD_{600} units of unlabeled cells and lysed in TNE buffer. Isolated total membranes were diluted with 1 vol of TNE and split into four fractions (500 μl) and subjected to a 30-min incubation with TX100 (1%) or buffer on ice. The samples then were adjusted to 40% Optiprep and overlaid with 30% Optiprep (2.3 ml, in TNE) and TNE buffer (0.5 ml) and centrifuged for 4 h at 28,000 rpm in a SW60 rotor. PLs were extracted from the top fraction (550 μl) according to ref. 22 and analyzed as described (21). SLs were extracted in 3 vol of chloroform/methanol/water/pyridine (60:30:6:1, vol/vol/vol/vol) overnight at room temperature and dried. Then, the samples were resuspended in 0.5 ml of chloroform/methanol/water (16:16:5, vol/vol/vol), saponified, and analyzed by TLC on silica plates with chloroform/methanol/4.2 M NH_3 (9:7:2, vol/vol/vol) as solvent. Sterols were labeled with 10 μCi of [^{14}C]acetate for 2 h and extracted and analyzed as for PLs. Radiolabeled lipids were visualized by autoradiography and quantified by PhosphorImager analysis (Molecular Dynamics).

Immunoblotting and Immunoprecipitation. The following antibodies were used for immunoblotting: rabbit anti-Gas1p (a gift of H. Riezman, University of Basel, Switzerland) at 1:20,000, rabbit anti-Pma1p (a gift of R. Serrano, Universidad Politecnica de Valencia, Spain) at 1:50,000, rabbit anti-Sec61p (a gift of E. Hurt, Heidelberg University, Germany) at 1:1,000, rabbit anti-α-agglutinin$^{20-351}$ (a gift of P. Lipke, University of New York) at 1:500, mouse anti-ALP (Molecular Probes) at 1:1,000, rabbit anti-PFK (a gift of J. Heinisch, Heinisch-Heine University, Düsseldorf, Germany) at 1:10,000, and mouse anti-V-H^+-ATPase (Molecular Probes) at 1:1,000. Immunoprecipitation of Gas1p and Pma1p was done as described (14, 23).

Acid Phosphatase Secretion. Cells (RH3804) were grown in yeast extract/peptone/dextrose medium at 24°C to log phase and washed once in distilled water and resuspended in 100 mM Tris, pH 9.4/50 mM 2-mercaptoethanol for 10 min. Then, cells were washed once in spheroplasting buffer (1.2 M sorbitol/10 mM KPi, pH 7.4) with 1% yeast extract and 2% bactopeptone (SB*) and resuspended in the same buffer at 20 OD_{600}/ml. Then, Zymolase 100T (0.1 mg/ml; ICN) was added, and, after a 30-min incubation at 24°C, cells were washed in SB* and resuspended in SB* at 10 OD_{600}/ml. Spheroplasts then were aliquoted for different time points (10 OD_{600}/time point) and spun down immediately before starting the incubation at 24°C or 37°C by adding 1 ml of fresh SB*. After incubating for 0, 30, 60 or 90 min, cells and medium were separated by centrifugation and acid phosphatase activity released to medium was assayed as in ref. 24.

Results

Isolation of DIGs from Yeast Cells. To explore the existence of functional rafts in the secretory pathway of budding yeast, we first developed a protocol for the isolation of DIGs. Cells (W303) were disrupted by using glass beads and the cleared lysate made 1% with respect to TX100 and incubated at 4°C for 30 min. The sample was adjusted to 40% Optiprep and loaded at the bottom of a step-density gradient (40%, 30%, 0% Optiprep). After centrifugation (2 h at 55,000 in TLS55 rotor), the DIG fraction was collected from the top of the gradient and subjected to a second incubation with TX100 and to density gradient centrifugation. Fractions from the second density gradient were collected from the top, and proteins were TCA-precipitated, separated by SDS/PAGE, and visualized by silver staining. This purification scheme allows the identification of proteins present in DIGs by their distribution along the density gradient; DIG-associated proteins are enriched at the top (fraction 1 in Fig. 1*a*) of the gradient. To identify protein components of DIGs we used a mass spectrometric approach in which in-gel cleavage of proteins with trypsin was followed by protein identification by MALDI peptide mapping and Nano ES MS/MS (21). Five candidate bands were identified successfully (Fig. 1). Only PMA1p, a 100-kDa protein, was identified by MALDI peptide mapping (10 peptides covered 15% of the sequence with mass accuracy better than 100 ppm). Although a sufficient amount of proteins was purified, only a few peptides were detected in the spectra of the in-gel digests of the other proteins, and, therefore, subsequent analysis by Nano ES MS/MS was required (Fig. 1). By mass spectrometry sequencing we have identified the plasma

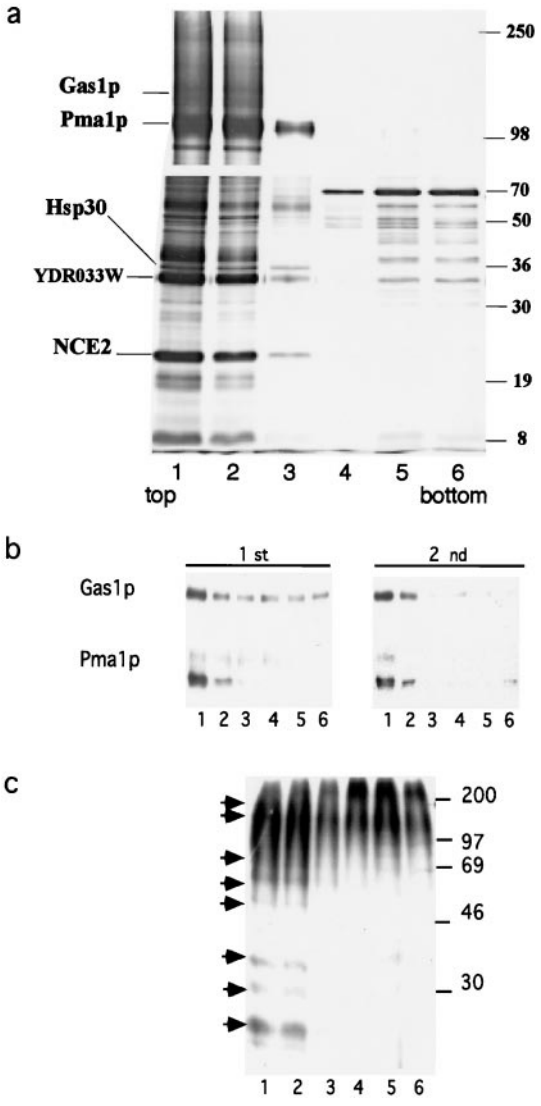

Fig. 1. Isolation of DIGs from yeast cells. (*a*) DIGs were enriched as described in *Materials and Methods*. Fractions of equal volume were collected from the top of the second gradient, TCA-precipitated, and analyzed by SDS/PAGE (7.5%, upper gel; 15%, lower gel) with silver staining. Proteins peaking at the top fractions were excised and sequenced by mass spectrometry. (*b*) Western blot analysis of Gas1p and Pma1p distribution in the first and second density gradients. (*c*) GPI-anchored proteins were labeled with [^{3}H]myoinositol (75 μCi) to steady-state. The cleared lysate was incubated with TX100 (1%) and adjusted to 40% Optiprep. The sample then was overlaid with a step gradient (30%, 0%) and centrifuged for 2 h at 55,000 (TLS55 rotor). Fractions collected from the top were TCA-precipitated and proteins were separated by SDS/PAGE (12.5%) and detected by autoradiography. The arrows indicate the position of DIG-associated protein bands.

membrane proton ATPase Pma1p, Gas1p, the tetra-spanning Nce2p, the seven-transmembrane-spanning Hsp30, and an unknown protein encoded by the ORF YDR033w, which is predicted to contain several transmembrane regions. Western blot analysis (Fig. 1*b*) of fractions from the first and second floatations showed that DIG-associated proteins were enriched by the second density gradient but not solubilized further, as indicated by their absence in the soluble (bottom) fractions. Our analysis thus demonstrated that the major plasma membrane proteins Pma1p and Gas1p are present in DIGs.

That GPI-anchored proteins undergo complex remodeling processes and can contain either ceramide or DAG-based anchors (25) prompted us to investigate whether the GPI anchor influences DIG association. To address this question, GPI-anchored proteins were labeled with [^{3}H]myoinositol, incubated with TX100 at 4°C, and floated once in a density gradient. The autoradiography of proteins separated by SDS/PAGE (Fig. 1*c*) showed that all of the bands detected were highly enriched in the DIG (top) fraction, indicating that both types of anchors lead to DIG association of GPI-anchored proteins. Gas1p, which, unlike the majority of GPI-anchored proteins contains a DAG-based anchor, was detected mainly in DIGs by Western blotting (see Fig. 1*b*) as shown above by mass spectrometry.

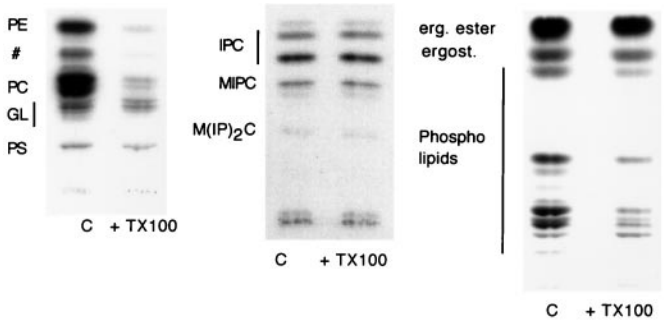

Fig. 2. TX100 solubility of total lipids in wild type (W303). Total floated membranes were incubated with TX100 or TNE buffer (c), adjusted to 40% Optiprep, and centrifuged in a density gradient as in Fig. 1. Lipids were extracted from the top fraction and analyzed by TLC. Labeled lipids were detected by autoradiography and quantified by phosphorimaging. PE, phosphatidylethanolamine; #, not assigned; PC, phosphatidylcholine; GL, glycolipids; PS, phosphatidylserine; IPC, inositol phosphorylceramide; MIPC, mannose-inositol-phosphorylceramide; $M(IP)_2C$, mannose-(inositol phosphorus)$_2$-ceramide.

SLs and Ergosterol but Not PLs Are Detergent Insoluble. To determine the lipid composition of the DIG fraction, cells (W303) were labeled either with [^{32}P]orthophosphate or [^{14}C]acetate and total floated membranes were incubated with TX100 (1% final) or buffer and floated once in a step-density gradient as before. Lipids were extracted from the top fraction and separated by TLC directly (PLs and ergosterol) or after alkaline hydrolysis (SLs) (see *Materials and Methods*). The pattern of bands found in the TX100-treated sample compared with the total (control) membrane fraction showed that whereas PLs were solubilized more than 90% (Fig. 2 *Left*), SLs and ergosterol (Fig. 2 *Center* and *Right*, respectively.) were mainly detergent-insoluble.

Ergosterol Depletion Disrupts DIGs. To investigate the requirement of ergosterol for DIG integrity, an ergosterol auxotroph mutant (*erg1*::*URA3*) (26) was grown in rich medium supplemented with cholesterol or ergosterol and unsaturated fatty acids. Washed cells were transferred to minimal medium with or without supplement and grown for 4 h to deplete sterols from membranes. After depletion, cells were lysed, treated with TX100, and floated in a density gradient as before. The DIG association of Gas1p and, to a lower extent, Pma1p was reduced in ergosterol-depleted compared with the sterol-supplemented cells (not shown).

To determine specifically the sterol requirement, ergosterol auxotroph cells (*erg12–1*) (27) were grown with cholesterol as supplement to replace ergosterol in membranes, thus allowing the later extraction of cholesterol using CD, which does not extract ergosterol efficiently (unpublished observation). Total membranes from cholesterol-grown cells were isolated by floatation and then incubated for 15 min at 37°C with buffer or increasing concentrations of CD. The membranes were pelleted

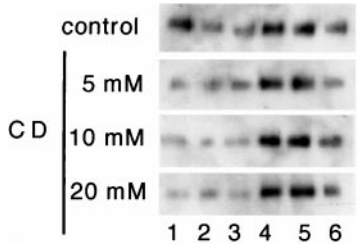

Fig. 3. DIG association in sterol-depleted membranes. *erg12–1* cells (GL7) were pregrown in medium supplemented with cholesterol. Total membranes were isolated by floatation and incubated with TNE buffer or TNE containing increasing concentrations of CD (0–20 mM) for 15 min at 37°C. Gas1p raft association was analyzed by Western blotting as in Fig. 1*b*.

to wash out CD, resuspended in buffer, and incubated with TX100 (1% final). After floatation in a density gradient, the distribution of Gas1p was analyzed by Western blotting (Fig. 3). Upon CD treatment the fraction of Gas1p present in DIGs is highly reduced. Essentially identical results were obtained by using the *erg1*::*URA3* mutant (not shown). We could also disrupt DIG association of Gas1p by depleting ergosterol from membranes of wild-type cells (W303) by using the polyene antibiotic nystatin (data not shown).

Sphingolipids Are Essential for DIG Integrity. Transport of GPI-anchored proteins from ER to Golgi is blocked in the *lcb1–100* temperature-sensitive mutant, which is deficient in ceramide synthesis, when incubated at the restrictive temperature (14). Using this mutant we analyzed the requirement of SLs for DIG integrity. Cells (*lcb1–100)* and wild type were grown in rich medium at the permissive temperature and then shifted to the restrictive temperature. Already at the permissive temperature, DIG association of Gas1p and Pma1p was reduced slightly in sphingolipid-mutant cells as compared with the wild type and totally impaired when shifted to the restrictive temperature for 2 h as indicated by the absence of both marker proteins in the DIG (top) fractions (Fig.4*a*). A similar effect was observed in cultures of the *lcb1–100* mutant grown in minimal medium overnight (not shown). When the temperature shift was done in a time course fashion, reduced DIG association of Gas1p was evident already after 30 min of incubation at the restrictive temperature (not shown).

To investigate whether sphingolipids are required for DIG association of ergosterol, *lcb1–100* and wild-type cells were labeled with [^{14}C]acetate for 2 h at 24°C or 37°C and the fraction of ergosterol present in DIGs was determined as before (see Fig. 2). At the permissive temperature both wild type and the *lcb1–100* mutant had ≈50% of ergosterol in DIGs, and this fraction is reduced significantly in the mutant but not in the wild type at the restrictive temperature (Fig. 4*b*), indicating that detergent insolubility of ergosterol requires sphingolipids.

Secretion of soluble acid phosphatase to the medium in the *lcb1–100* mutant, although reduced, was not abolished after shifting to a nonpermissive temperature for different periods of time (Fig. 4*c*).

DIG Association Takes Place at the Level of the ER. That the absence of ceramide synthesis blocks ER-to-Golgi transport of GPI-anchored proteins (13, 14) prompted us to investigate whether DIG association is acquired already at the level of the ER or later in the Golgi as in mammalian cells. First, we examined the DIG association of α-agglutinin, which exhibits a dramatic change in size because of extensive glycosylation in the ER and the Golgi (28). After induction of its synthesis by mixing cells of both mating types, both the ER (80 and 140 kDa) and the plasma

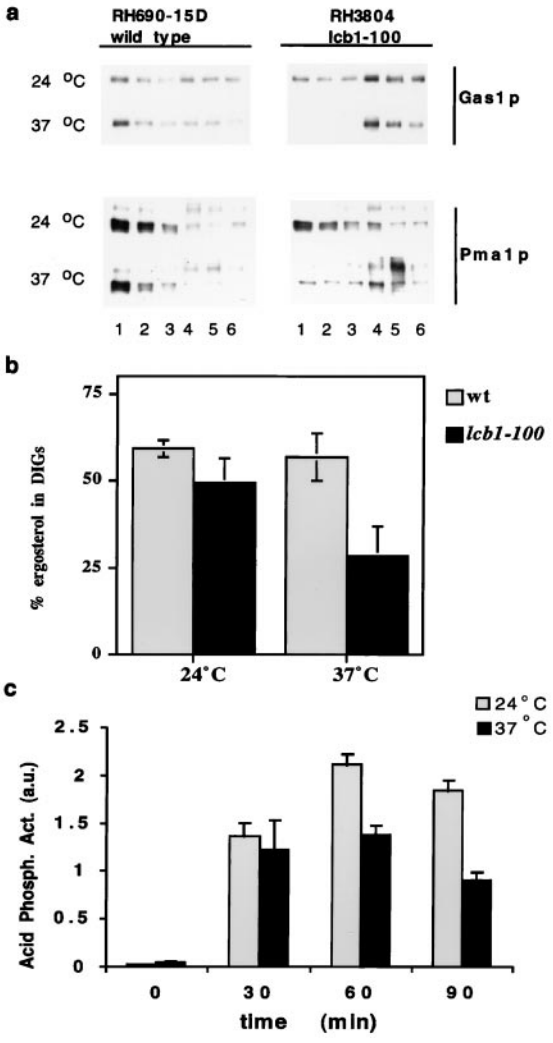

Fig. 4. DIG association in SL depleted cells. (*a*) Wild-type (RH690–15D) and *lcb1–100* cells (RH3804) were grown in rich medium at 24°C. The cultures were split and incubated for 2 h at 24°C or 37°C. DIG association was analyzed by Western blotting after TX100 treatment and density gradient centrifugation (fraction 1, *Upper*; fraction 6, *Lower*). (*b*) Wild-type (RH690–15D) and *lcb1–100* cells (RH3804) were labeled with [^{14}C]acetate for 2 h (in NaPi + 1% glucose) at 24°C or 37°C. Ergosterol insolubility was determined by TLC analysis as in Fig. 2 (n = 3). (*c*) Secretion of acid phosphatase to the medium in spheroplasted *lcb1–100* cells incubated at 24°C or 37°C (n = 4), expressed in arbitrary units.

membrane forms (>250 kDa) were found in the DIG fraction (not shown). Next, we checked whether non-GPI-anchored proteins that are DIG-associated also become detergent-insoluble in the ER. To do so, we used the *sec18–1* temperature-sensitive mutant (29), which imposes a general ER-to-Golgi block, and performed a pulse–chase experiment at permissive and restrictive temperatures. DIG association of [^{35}S]methionine-labeled proteins was monitored by the acquisition of detergent insolubility by subjecting aliquots from different time points to two incubations with TX100 and density gradient centrifugations. Already at the beginning of the chase, after a short (5-min) pulse labeling, proteins were found in the DIG fractions at both temperatures (not shown). We then analyzed the association of Gas1p with DIGs during biosynthetic transport. The acquisition of TX100 insolubility was followed by performing a pulse–chase experiment in *sec18–1* mutant and wild-type cells. Aliquots for two different time points were subjected to TX100 extraction and density gradient centrifuga-

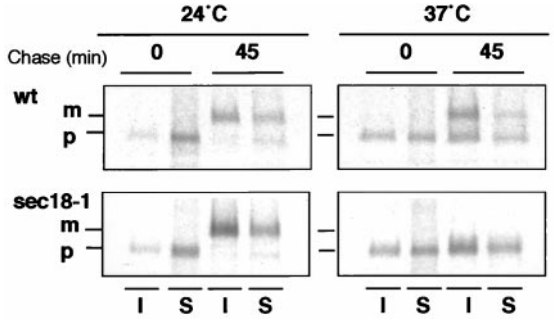

Fig. 5. DIG association of Gas1p during biosynthetic transport. Cells [wild type (NY179) and *sec18–1* (H891)] were preincubated at 24°C or 37°C for 5 min, pulse-labeled with [^{35}S]methionine for 5 min, and then chased for 0 and 45 min. The samples from the two time points were taken and subjected to TX100 extraction and density gradient centrifugation. Gas1p was immunoprecipitated from fractions 1 [insoluble (I)] and 4 [soluble (S)]; the mature (m) and precursor (p) forms are indicated.

tion (once), and Gas1p was immunoprecipitated from the gradient fractions. Gas1p started to become insoluble in the ER as indicated by the presence of the 105-kDa (precursor) form in the DIG fraction. The association with DIGs was increased significantly for the 125-kDa (mature) form at 24°C, both in the wild type and in *sec18–1* cells, or for the precursor form after 45 min at 37°C in the *sec18–1* mutant (see Fig. 5). These data demonstrate that in contrast to mammalian cells, DIG association starts in the ER in yeast.

A Subset of Surface Proteins but Not ER Resident or Vacuolar Membrane Proteins Are DIG-Associated. We have demonstrated that a number of cell surface proteins become DIG-associated in the ER. To find out whether other membrane proteins also become TX100-insoluble, we tested two vacuolar membrane proteins, alkaline phosphatase and V-H$^+$ATPase (100-kDa subunit). Both vacuolar proteins were fully soluble after incubation with TX100 (Fig. 6*a*) as was Sec61p, an ER permanent resident membrane protein. Depletion of SLs blocks ER-to-Golgi transport of GPI-anchored proteins but does not block CPY transport to the vacuole nor secretion of soluble markers (refs. 13–15 and this work). To analyze whether there are proteins in the plasma membrane that are not in DIGs, we expressed hTfR, a non-raft marker commonly used in mammalian cells (5) that has been shown to be localized at the plasma membrane when expressed in yeast (30). All of the hTfR was membrane associated, floating with Gas1p in density gradients without TX100, but hTfR was fully soluble upon treatment with TX100 (Fig. 6*b*).

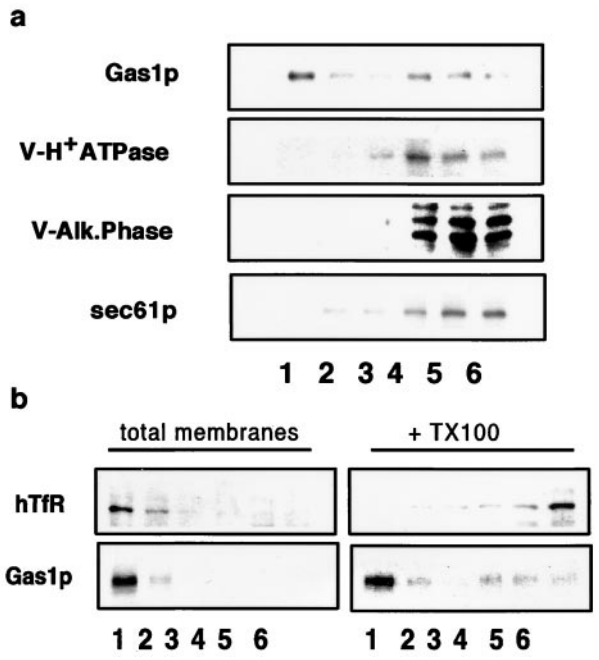

Fig. 6. DIG association of vacuolar, ER, and plasma membrane proteins. (*a*) DIG association of Gas1p, V-H$^+$ATPase (100-kDa subunit), V-ALP, and Sec61p in wild-type (W303) cells was analyzed as in Fig. 1 by Western blotting with specific antibodies. (*b*) hTfR was expressed in wild-type (W303) cell membranes, and DIG association was analyzed by floatation in density gradients as in Fig. 1 with or without TX100 treatment.

Discussion

In this study we have investigated the presence of lipid rafts in the yeast *Saccharomyces cerevisiae.* By exploiting their insolubility in cold TX100, we have been able to isolate glycosphingolipid and ergosterol-rich membrane domains from yeast cells by density gradient centrifugation. The procedure we have developed allowed us to examine both the lipid and protein composition of DIGs. After two successive density gradient centrifugations, DIG-associated proteins can be seen as distinct bands peaking at the top of the second gradient, clearly distinguishable from other proteins that are soluble in TX100 or insoluble material such as cytoskeletal elements.

Several lines of evidence indicate that the proteins identified by mass spectrometry (Pma1p, Gas1p, Hsp30, and Nce2p) are specifically DIG-associated. GPI-anchored proteins such as Gas1p are found in DIGs in mammalian cells (4). Also, in yeast all GPI-anchored proteins we could detect by inositol labeling were DIG-associated (Fig. 1*c*). Moreover, SLs and ergosterol depletion impair DIG association of Gas1p and Pma1p (Figs. 3 and 4*a*) (see below). In addition, Hsp30 has been shown to interact with Pma1p (31). These results are in contradiction with a previous report showing the existence of a TX100-insoluble fraction in yeast from which Gas1p and Pma1p were excluded (16). Most likely, the apparent lack of lipid association of both of these markers arose from the pelleting step before the floatation in sucrose. When total membranes are pelleted from the cleared lysate, the pellet contains remainders of cell walls, debris, and cytoskeletal elements, resulting in the trapping of material that otherwise would have a lower density.

Analysis of the lipid composition of the DIG fraction (Fig. 2) shows a high enrichment of ergosterol, and of SLs in DIGs, and a depletion of PLs, of which less than 10% were DIG-associated with the remarkable exception of phosphatidylserine (PS), which is much more resistant to TX100 extraction. Consistent with the raft hypothesis (2), the PS found in the plasma membrane of yeast has the highest level of saturation among the PLs (10) and, therefore, a stronger tendency to associate with rafts (32). One interesting feature of the yeast plasma membrane that is derived from our results is the very high proportion of ergosterol and SLs found in DIGs. In the yeast plasma membrane at least two lipid phases are present, as suggested by the differential solubility of markers for raft (Pma1p, Gas1p) and nonraft (hTfR) proteins (Fig. 6*b*). In agreement with this, studies of phase transitions in isolated yeast plasma membranes are consistent with the existence of sterol-rich and sterol-poor phases (33). The high sterol and SL-to-PL ratio present in the plasma membrane of yeast is characteristic for specialized membranes that are exposed to the external environment and thus are under high stress, such as the apical membrane of epithelial cells (1). In these membranes the raft lipids seem to form the major lipid phase. According to this view, sorting of lipids to the yeast plasma membrane and to the apical membrane of MDCK cells may show similar properties.

Early Segregation of Proteins in the Secretory Pathway. Incorporation of proteins into DIGs in mammalian cells takes place in the Golgi complex (3, 5), where the lipid building blocks of rafts first coincide. In yeast, DIGs form earlier, already in the ER (see Fig. 5), where inositol phosphorylceramide is first found (34). Alternatively, ceramide itself could be able to supply the function of SLs in the ER by means of its very long fatty acid (35). However, whether ceramide associates with DIGs is a question that remains to be investigated. Interestingly, the fraction of Gas1p associated with DIGs became significantly higher for the mature form (post-ER) (Fig. 5), suggesting that rafts could be more stable once the more complex SLs are incorporated. It is important to note that ER resident proteins or proteins targeted to an ergosterol/SL-poor membrane, such as the vacuole, are excluded from raft microdomains (Fig. 6*a*). Thus, the raft route seems to lead to the plasma membrane in biosynthetic traffic.

The early assembly of DIGs in the secretory pathway leads to the prediction that different populations of COPII vesicles bud from the ER—those that transport raft proteins and those that do not. Previous results have shown that SLs are required for Gas1p transport from the ER to the Golgi but not for secretory and not for vacuolar proteins (13, 14). This segregation seems to be kept en route to the surface because two different populations of post-Golgi vesicles can be isolated after blocking transport to the plasma membrane (36). To understand this process and the involvement of lipid rafts in the formation of post-Golgi transport containers, a careful characterization of their lipid and protein composition is needed.

A number of genetic screens have uncovered a wide set of genes involved in the secretory function (29). However, little is known about the sorting mechanisms responsible for plasma membrane delivery. The length of the hydrophobic transmembrane domain has been shown both in mammalian cells and yeast to be important for Golgi retention and plasma-membrane targeting (37, 38). En route to the surface, ergosterol and SLs are enriched progressively, together with highly saturated phospholipid species, increasing bilayer thickness. Thus, the idea that proteins with longer hydrophobic peptide segments prefer thicker membranes (39) is in agreement with the concept of rafts as sorting platforms.

We thank W. David Ness and Leo Parks for providing strains and Peter Lipke, Ramon Serrano, Wolfgang Zachariae, and Ed Hurt for antibodies. We are especially grateful to Howard Riezman for the gift of antibodies and strains and for instructive advice. We also thank Fedor Severin and W. Zachariae for advice during the course of this work and Kim Ekroos for technical assistance. This work was supported by a European Union network grant, a grant from the Deutsche Forschungsgemeinschaft (SFB352), and a grant from the Academy of Finland (8244).

1. Simons, K. & van Meer, G. (1988) *Biochemistry* **27,** 6197–6202.
2. Simons, K. & Ikonen, E. (1997) *Nature* (London) **387,** 569–572.
3. Brown, D. A. & London, E. (1998) *J. Membr. Biol.* **164,** 103–114.
4. Brown, D. A. & Rose, J. K. (1992) *Cell* **68,** 533–544.
5. Scheiffele, P., Roth, M. G. & Simons, K. (1997) *EMBO J.* **16,** 5501–5508.
6. Keller, P. & Simons, K. (1998) *J. Cell Biol.* **140,** 1357–1367.
7. Ledesma, M. D., Simons, K. & Dotti, C. (1998) *Proc. Natl. Acad. Sci. USA* **95,** 3966–3971.
8. Mays, R. W., Siemers, K, Fritz, B., Lowe, A., van Meer, G. & Nelson, W. J. (1995) *J. Cell Biol.* **130,** 1105–1115.
9. Zinser, E., Paltauf, F. & Daum, G. (1993) *J. Bacteriol.* **175,** 2853–2858.
10. Schneiter, R., Brugger, B., Sandhoff, R., Zellnig, G., Leber, A., Lampl, M., Athenstaedt, K., Hrastnik, C., Eder, S., Daum, G., *et al.* (1999) *J. Cell Biol.* **146,** 741–754.
11. Zinser, E., Sperka-Gottlieb, C. D. M., Fasch, E., Kohlwein, S. D, Paltauf, F. & Daum, G. (1991) *J. Bacteriol.* **173,** 2026–2034.
12. Hechtberger, P., Zinser, E., Saf, R., Hummel, K., Paltauf, F. & Daum, G. (1994) *Eur. J. Biochem.* **225,** 641–649.
13. Hovarth, A., Sütterlin, C., Manning-Krieg, U., Movva, N. R. & Riezman, H. (1994) *EMBO J.* **13,** 3687–3695.
14. Sütterlin, C., Doering, T., Schimmöller, F., Schröder, S. & Riezman, H. (1997) *J. Cell Sci.* **110,** 2703–2714.
15. Skrzypek, M., Lester, R. L. & Dickson, R. C. (1997) *J. Bacteriol.* **179,** 1513–1520.
16. Kubler, E., Dohlman, H. G. & Lisanti, M. P. (1996) *J. Biol. Chem.* **271,** 32975–32980.
17. Sherman, F. (1991) *Methods Enzymol.* **194,** 3–21.
18. Warner, J. R. (1991) *Methods Enzymol.* **194,** 423–428.
19. Shevchenko, A., Jensen, O. N., Podtelejnikov, A. V., Sagliocco, F., Wilm, M., Vorm, O., Mortensen, P., Boucherie, H. & Mann, M. (1996) *Proc. Natl. Acad. Sci. USA* **93,** 14440–14445.
20. Wilm, M., Shevchenko, A., Houthaeve, T., Breit, S., Schwegerer, L., Fotsis, T. & Mann, M. (1996) *Nature (London)* **379,** 466–469.
21. Scheiffele, P., Rietveld, A., Wilk, T. & Simons, K. (1999) *J. Biol. Chem.* **274,** 2038–2044.
22. Bligh, E. G. & Dyer, W. J. (1959) *Can. J. Biochem. Physiol.* **37,** 911–917.
23. Chang, A. & Slayman, C. W. (1991) *J. Cell Biol.* **115,** 289–295.
24. Van Rijn, H. J. M., Boer, P. & Steyn-Parve, E. P. (1972) *Biochim. Biophys. Acta.* **268,** 431–441.
25. Frankhauser, C., Homans, S. W., Thomas-Oates, J. E., McConville, M. J., Despons, C., Cozelmann, A. & Ferguson, M. A. J. (1993) *J. Biol. Chem.* **268,** 26365–26374.
26. Tomeo, M. E., Fenner, G., Tove, S. R. & Parks, L. (1992) *Yeast* **8,** 1015–1024.
27. Venkatramesh, M., Guo, D., Jia, Z. & Nes, W. D. (1996) *Biochim. Biophys. Acta.* **1259,** 313–324.
28. Lu, C., Kurjan, J. & Lipke, P. N. (1994) *Mol. Cell Biol.* **14,** 4825–4833.
29. Novick, P., Field, C. & Scheckman, R. (1980). *Cell* **21,** 205–215.
30. Terng, H., Gessner, R., Fuchs, H., Stahl, U. & Lang, C. (1998) *FEMS Microbiol. Lett.* **160,** 61–67.
31. Braley, R. & Piper, P. W. (1997) *FEBS Lett.* **418,** 123–126.
32. Schroeder, R., London, E. & Brown, D. (1994) *Proc. Natl. Acad. Sci. USA* **91,** 12130–12134.
33. Bottema, C. D. K., McLean-Bowen, C. A. & Parks, L. (1983) *Biochim. Biophys. Acta.* **734,** 235–248.
34. Puotti, A., Despons, C. & Conzelmann, A. (1991) *J. Cell Biol.* **113,** 515–525.
35. Muñiz, M. & Riezman, H. (2000) *EMBO J.* **19,** 10–15.
36. Harsay, E. & Bretscher, A. (1995) *J. Cell Biol.* **131,** 297–310.
37. Munro, S. (1995) *EMBO J.* **14,** 4695–4704.
38. Rayner, J. C. & Pelham, H. R. (1997) *EMBO J.* **16,** 1832–1841.
39. Bretscher, M. S. & Munro, S. (1993) *Science* **261,** 1280–1288.